

Extreme events in solutions of hydrostatic and non-hydrostatic climate models

J. D. Gibbon and D. D. Holm

Department of Mathematics, Imperial College London, London SW7 2AZ, UK

Contents

1	Review of the hydrostatic & non-hydrostatic primitive equations	2
2	Formulating the Primitive Equations	5
2.1	Hydrostatic primitive equations (HPE)	6
2.2	Non-hydrostatic primitive equations (NPE)	8
3	Extreme events & their interpretation	9
3.1	Proof of Theorem 1	11
3.1.1	The evolution of the enstrophy	11
3.1.2	The evolution of $\int_V \Theta_z ^2 dV$	15
3.1.3	A combination of the fluid and temperature inequalities	17
4	Potential implications for simulations	19

Abstract

Initially this paper reviews the mathematical issues surrounding the hydrostatic (HPE) and non-hydrostatic (NPE) primitive equations that have been used extensively in numerical weather prediction and climate modelling. Cao and Titi (2005, 2007) have provided a new impetus to this by proving existence and uniqueness of solutions of viscous HPE on a cylinder with Neumann-like boundary conditions on the top and bottom. In contrast, the regularity of solutions of NPE remains an open question. With this HPE regularity result in mind, the second issue examined in this paper is whether extreme events are allowed to arise spontaneously in their solutions. Such events could include, for example, the sudden appearance and disappearance of locally intense fronts that do not involve deep convection. Analytical methods are used to show that for viscous HPE, the creation of small-scale structures is allowed locally in space and time at sizes that scale inversely with the Reynolds number.

A review dedicated to the memory of Robin Bullough.

1 Review of the hydrostatic & non-hydrostatic primitive equations

The hydrostatic primitive equations (HPE) were developed more than eighty years ago by Richardson as a model for large-scale oceanographic and atmospheric dynamics [1]. In various forms they have been the foundation of most numerical weather, climate and global ocean circulation predictions for many decades. The HPE govern incompressible, rotating, stratified fluid flows that are in hydrostatic balance. This balance is broken, however, in *deep convection* which occurs in cloud formation, flows over mountains and vertical fluid entrainment by strong gravity currents¹. In this context, the *hydrostatic approximation* is the most reliable and accurate of all the assumptions made in applying them to operational numerical weather prediction (NWP), climate modelling and global numerical simulations of ocean circulation. The approximation arises from a scale analysis of synoptic systems; see [2, 3, 4, 5, 6, 7, 8, 9, 10, 11, 12, 13, 14, 15, 16, 17, 18]. Basically, it neglects the vertical acceleration term in the vertical momentum equation. Physically, this enforces a perfect vertical force balance between gravity and the vertical pressure gradient force, which means that the pressure at a given location is given by the weight of the fluid above.

Until recently, the resolution of operational NWP models has been limited by computing power and operational time constraints on resolutions in which the hydrostatic approximation is almost perfectly valid. Operational forecasts therefore have relied mainly on hydrostatic models, which applied extremely well in numerical simulations of the global circulation of both the atmosphere and the ocean at the spatial and temporal resolutions that were available at the time. In parallel, the development of non-hydrostatic atmospheric models, which retain the vertical acceleration term and thus capture strong vertical convection, has also been pursued over a period of more than four decades, especially for mesoscale investigations of sudden storms. As computer systems have become faster and memory has become more affordable over the past decade, there has been a corresponding increase in the spatial resolution of both NWP and climate simulation models. This improvement has facilitated a transition from highly developed hydrostatic models towards non-hydrostatic models. Over the past decade, atmospheric research institutions have begun replacing their operational hydrostatic models with non-hydrostatic versions [14, 15, 17].

An impending 'model upgrade' may be tested by comparing the solution properties of the existing hydrostatic model at a new higher resolution with those of its non-hydrostatic alternative (NPE). Using the fastest supercomputers available, global simulations of atmospheric circulation at resolutions of about 10 km in the horizontal (in the region of the hydrostatic limit) have recently been performed [19, 20]. In the past these simulations have been carried out using only hydrostatic models, as the non-hydrostatic versions were still under development. Perhaps not unexpectedly, the simulations at finer resolution found much more fine-scale structure than had been seen previously. More importantly, the smallest coherent features found at the previous coarser limits of resolution were no longer present at new finer resolutions, because the balance between nonlinearity and dissipation that had created them previously was no longer being enforced. Instead, it was being enforced at the new limits of resolution.

¹The subtle difference is explained in §2 between what is known as modellers' HPE (MHPE) pioneered by Richardson and incorporated in many numerical weather prediction and climate simulation models, and HPE in cartesian geometry discussed here.

Consequently, an important conclusion from these PE simulations has been that the transition from the existing hydrostatic model to its non-hydrostatic alternative, and the distinction between their solutions, will require in both cases a much better understanding of the formation of fine-scale frontal structures [20, 21]. For discussions of the history of ideas in fronto-genesis see [22, 23, 25, 24]. An example of fine-scale wind measurements is a ‘gust front’ are found in Figure 1 [16, 26, 27]. Gust fronts are indicated by ‘bow echoes’ on Döppler radar. These have been extensively observed and studied as the precursors of severe local weather.

In particular, the physical parameterizations in hydrostatic models are likely to require dramatic changes when simulated at new finer resolutions. Therefore, in order to obtain the full benefit of the potential increase in accuracy provided by such high spatial resolution when using the non-hydrostatic model, one must first determine the range of solution behavior arising at the finer resolution in the computations of the previous hydrostatic model [20]. Over relatively small domains, operational model resolutions in the atmosphere are in fact already beyond the hydrostatic limit. These models run at resolutions finer than 10 km , where convection is partially resolved (thus, inaccurately simulated) by non-hydrostatic models. However, convection can only be fully resolved at model resolutions of about two orders of magnitude finer, that is, about 100 m or less in the horizontal. It is therefore likely that, for many years to come, operational hydrostatic and non-hydrostatic models will function at resolutions where convection can only be partially resolved. Consequently, the distinction between hydrostatic and non-hydrostatic solution behavior at these intermediate resolutions becomes paramount for the accuracy, predictability, reliability and physical interpretation of results in NWP.

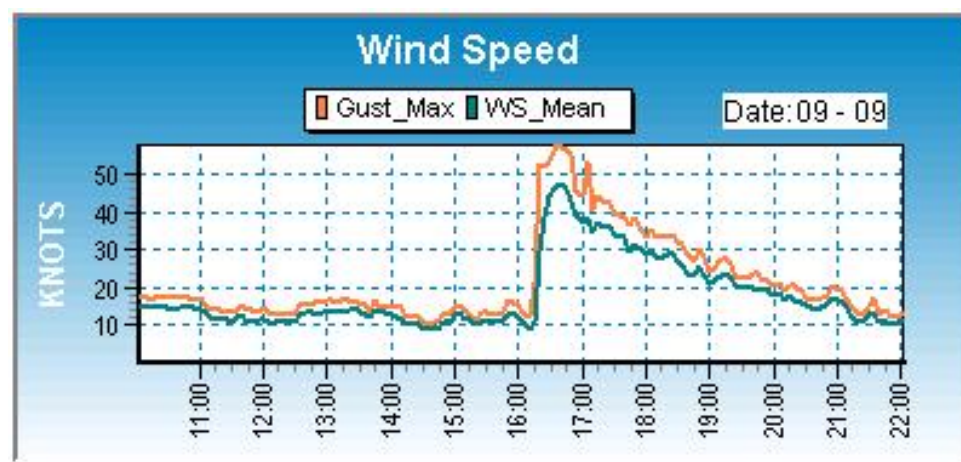


Figure 1: An example of a gust front manifesting itself in a sudden rise in wind speed [16, 26].

Against this background of renewed interest in the improvement of hydrostatic models and their newly acquired computability at higher resolution, this paper also reviews the development of new mathematical ideas introduced by Cao and Titi [28, 29], who have proved the existence and uniqueness of *strong* solutions of the viscous hydrostatic primitive equations². The corresponding regularity problem for viscous NPE remains open³. Ju [33] then built on the result of Cao and Titi to show

²See also Kobelkov [30, 31, 32] for a subsequent independent method.

³This is closely related to the open regularity problem for the three-dimensional Navier-Stokes equations which has been solved only for very thin domains ($0 < \alpha_a \ll 1$): see [34, 35, 36].

that the viscous HPE actually possess a global attractor, which means that the bounds are constants although no explicit estimates were given. The status of results prior to the Cao and Titi proof [28, 29] (e.g. the existence of weak solutions) can be found in the papers by Lions, Temam and Wang [37, 38, 39] and Lewandowski [40]. Considering the technical difficulties of this new work, which has been solved on a cylindrical domain with Neumann-type boundary conditions on the top and bottom, these results must be classed as a major advance⁴. The significance of this result in establishing the existence and uniqueness of strong solutions of viscous HPE is that **no singularities of any type can form in the solutions**.

The title and abstract of this review refer to the idea of ‘extreme events’: this term should not be interpreted in the present context in a statistical sense, but as the spontaneous appearance and disappearance of local, sudden, intermittent events with large gradients in the atmosphere or the oceans. These events would register as spatially localized, intense concentrations of vorticity and strain. Until the the Cao-Titi result, a major open question in the subject had been whether these strong variations ultimately remained smooth? Now that we know that solutions of HPE must remain smooth at every scale, the question still remains whether this smoothness precludes the existence of extreme events representing front-like structures: this would be manifest in jumps or steep gradients in double mixed derivatives such as $|\partial^2 u_1 / \partial x_2 \partial x_3|$ or $|\partial^2 u_2 / \partial x_1 \partial x_3|$ within *finite* regions of space-time. The ultimate aim is to explain fine-structure processes such as those that occur in fronto-genesis: see the work of Hoskins [23, 24] and Hoskins and Bretherton [25] for general background on this phenomenon.

§3 of this paper seeks to address this problem from a mathematical angle. The regularity of solutions opens a way of showing that front-like events are possible at very fine scales. The method used is to search for fine structure by examining the local behaviour of solutions in space-time. The conventional approach to PDEs has been to prove bounded-ness of norms which, as volume integrals, tend to obscure the fine structure of a solution. The idea was first used (under strong regularity assumptions) to estimate intermittency in Navier-Stokes turbulence [41]. The mathematical approach is to show that solutions of HPE may be divided into two space-time regions \mathbb{S}^+ and \mathbb{S}^- . If \mathbb{S}^- is non-empty then *very large lower bounds* on double mixed derivatives of components of the velocity field (u_1, u_2, u_3) such as $|\partial^2 u_1 / \partial x_2 \partial x_3|$ or $|\partial^2 u_2 / \partial x_1 \partial x_3|$ may occur within \mathbb{S}^- . These large point-wise lower bounds on second-derivative quantities represent intense accumulation in the (x_1, x_3) - and (x_2, x_3) -planes, respectively. Clearly, if solutions of great intensity were to accumulate in regions of the space-volume, this could only be allowed for finite times, in local spatial regions. Thus one would see the spontaneous formation of a front-like object localised in space that would only exist for a finite time. More specifically, the lower bounds within \mathbb{S}^- referred to above are a linear sum of $\mathcal{R}_{u_{hor}}^6$, $\mathcal{R}_{u_3}^6$ and $\mathcal{R}_{a,T}^6$ where $\mathcal{R}_{u_{hor}}$ and \mathcal{R}_{u_3} are *local* Reynolds numbers. That is, they are defined using the local space-time values of $u_{hor}(x_1, x_2, x_3, \tau) = \sqrt{u_1^2 + u_2^2}$ and the vertical velocity $u_3 = u_3(x_1, x_2, x_3, \tau)$. Likewise, $\mathcal{R}_{a,T}$ is a local Rayleigh number, defined using the local temperature $T(x_1, x_2, x_3, \tau)$. In contrast, Re is the global Reynolds number. These lower bounds within the \mathbb{S}^- -regions can be converted into lower bounds on the two point-wise inverse length scales λ_H

$$L\lambda_H^{-1} > c_{u_{hor}} \mathcal{R}_{u_{hor}} + c_{u_3} \mathcal{R}_{u_3} + c_{1,T} \mathcal{R}_{a,T} + c_{2,T} Re^{2/3} \mathcal{R}_{a,T}^{1/3} + \text{forcing}. \quad (1.1)$$

⁴Unfortunately the methods used for HPE do not extend to the three-dimensional Navier-Stokes equations; although HPE had been thought to be the more difficult of the two. See Lions, Temam and Wang [37, 38, 39].

The term $\mathcal{R}_{u_3} \sim O(\varepsilon)$ is negligible compared to $\mathcal{R}_{u_{hor}}$ because regions of strong vertical convection are absent in HPE. If such a result were valid for NPE, it would be this vertical term that would be restored. The estimate for λ_H in (1.1) is of the order of a *metre* or less, at high Reynolds numbers. Our interpretation of this very small length is not that it is necessarily the thickness of a front, but that it may refer to the smallest scale of features *within* a front. If an equivalent result for NPE could be found then the estimate of the length-scale λ_N (say) would likely be considerably smaller than that for λ_H .

2 Formulating the Primitive Equations

Quantity	Symbol	Definition
Typical horizontal length	L	
Typical vertical length	H	
Typical temperature	T_0	
Aspect ratio	α_a	$\alpha_a = H/L$
Typical velocity	U_0	
Twice vertical rotation rate	f	
Global Reynolds number	Re	$Re = U_0 L \nu^{-1}$
Rossby number	ε	$\varepsilon = U_0 (L f)^{-1}$
Rayleigh number	R_a	$R_a = g \alpha T_0 H^3 (\nu \kappa)^{-1}$
Hydrostatic const	a_0	$a_0 = \varepsilon \sigma \alpha_a^{-3} R_a Re^{-2}$
Frequency	ω_0	$\omega_0 = U_0 L^{-1}$

Table 1: Definition of symbols for the primitive equations.

In what follows, *dimensionless* co-ordinates are denoted by (x, y, z, t) . These are related to *dimensional* variables (x_1, x_2, x_3, τ) through the horizontal length scale L , the vertical length scale H : Table 1 gives the various standard definitions. Table 2 gives the notation concerning dimensionless and dimensional variables and some of the relations between them.

Dimensionless versions of both the HPE and NPE are expressed in terms of a set of velocity vectors based on the two horizontal velocities (u, v) and the vertical velocity w . These form the basis for the three-dimensional vector⁵

$$\mathbf{V}(x, y, z, t) = (u, v, \varepsilon w), \quad (2.1)$$

satisfying $\text{div } \mathbf{V} = 0$ or $u_x + v_y = -\varepsilon w_z$. The hydrostatic velocity vector is defined by

$$\mathbf{v} = (u, v, 0), \quad (2.2)$$

and the non-hydrostatic velocity vector by

$$\mathbf{v} = (u, v, \alpha_a^2 \varepsilon w), \quad (2.3)$$

⁵Comparing with the notation in [9], $(u, v) \equiv \mathbf{u}_2$ while $\mathbf{V} \equiv \mathbf{u}_3$ and $\mathbf{v} \equiv \mathbf{v}_3$.

	<i>Dimensionless</i>	<i>Dimensional</i>	<i>Relation</i>
Horiz co-ords	x, y	x_1, x_2	$(x, y) = (x_1, x_2)L^{-1}$
Vertical co-ord	z	x_3	$z = x_3H^{-1}$
Time	t	τ	$t = \tau U_0 L^{-1}$
Horiz velocities	(u, v)	$\mathbf{u} = (u_1, u_2)$	$(u, v) = (u_1, u_2)U_0^{-1}$
Vertical velocity	w	u_3	$\varepsilon U_0 \alpha_a w = u_3$
Velocity vector	$\mathbf{V} = (u, v, \varepsilon w)$		
Hydro-Velocity	$\mathbf{v} = (u, v, 0)$		
Non-Hydro-Vel	$\mathbf{v} = (u, v, \alpha_a^2 \varepsilon w)$		
Temperature	Θ	T	$\Theta = TT_0^{-1}$
2D-Gradient	$\nabla_2 = \mathbf{i}\partial_x + \mathbf{j}\partial_y$		
3D-Gradient	$\nabla_3 = \mathbf{i}\partial_x + \mathbf{j}\partial_y + \mathbf{k}\partial_z$	$\nabla = \mathbf{i}\partial_{x_1} + \mathbf{j}\partial_{x_2} + \mathbf{k}\alpha_a\partial_{x_3}$	$\nabla_3 = L\nabla$
3D-Laplacian	$\Delta_3 = \partial_x^2 + \partial_y^2 + \partial_z^2$		
Vorticity	$\boldsymbol{\omega} = \text{curl } \mathbf{V}$	$\boldsymbol{\Omega}$	$\Omega_3 = \omega_3\omega_0$
Hydro-vorticity	$\boldsymbol{\zeta} = \text{curl } \mathbf{v}$		
Non-hydro-vorticity	$\mathbf{w} = \text{curl } \mathbf{v}$		
Heat transport	q	Q	

Table 2: Connection between dimensionless & dimensional variables.

where α_a is the aspect ratio defined in Table 3. Neither \mathbf{v} nor \mathbf{v} are divergence-free.

The HPE that are studied in this paper should be compared with the modellers' HPE (MHPE) used by Richardson and incorporated in many numerical weather prediction and climate simulation models to this day [14, 15, 16, 17]. While the MHPE are written for a compressible fluid in the non-Euclidean geometry of a shallow atmosphere (i.e. the domain of flow is a spherical shell of constant radius, although vertical extent and motion are allowed) the HPE as laid out in Section 2.1 are written for an incompressible fluid in a Cartesian geometry. The 'incompressibility' of hydrostatic models appears when pressure is used as vertical coordinate. Hoskins and Bretherton [25] used a function of pressure to define a vertical coordinate that delivers the hydrostatic primitive equations for a compressible fluid that are nearly isomorphic to those for an incompressible fluid when ordinary height is used as vertical coordinate. They then introduced an approximation in the continuity equation that made the near isomorphism exact. The resulting HPE have frequently been used in theoretical studies and have led to many important results, but they are not identical to the MHPE that numerical modellers since Richardson have typically used.

2.1 Hydrostatic primitive equations (HPE)

The HPE in dimensionless form for the two horizontal velocities u and v are

$$\varepsilon \left(\frac{\partial}{\partial t} + \mathbf{V} \cdot \nabla_3 \right) u - v = \varepsilon Re^{-1} \Delta_3 u - p_x, \quad (2.4)$$

and

$$\varepsilon \left(\frac{\partial}{\partial t} + \mathbf{V} \cdot \nabla_3 \right) v + u = \varepsilon Re^{-1} \Delta_3 v - p_y. \quad (2.5)$$

There is no evolution equation for the vertical velocity w which lies in both $\mathbf{V} \cdot \nabla_3$ and the incompressibility condition $\text{div } \mathbf{V} = 0$. The z -derivative of the pressure field p and the dimensionless temperature Θ enter the problem through the hydrostatic equation

$$a_0 \Theta + p_z = 0, \quad (2.6)$$

where a_0 is defined in Table 1. The hydrostatic velocity field $\mathbf{v} = (u, v, 0)$ appears when (2.4), (2.5) and (2.6) are combined

$$\varepsilon \left(\frac{\partial}{\partial t} + \mathbf{V} \cdot \nabla_3 \right) \mathbf{v} + \mathbf{k} \times \mathbf{v} + a_0 \mathbf{k} \Theta = \varepsilon Re^{-1} \Delta_3 \mathbf{v} - \nabla_3 p, \quad (2.7)$$

and taken in tandem with the incompressibility condition $\text{div } \mathbf{v} = -\varepsilon w_z$. The dimensionless temperature⁶ Θ , with a specified heat transport term $q(x, y, z, t)$, satisfies

$$\left(\frac{\partial}{\partial t} + \mathbf{V} \cdot \nabla_3 \right) \Theta = (\sigma Re)^{-1} \Delta_3 \Theta + q. \quad (2.8)$$

The chosen domain is a cylinder of height H ($0 \leq z \leq H$) and radius L , designated as $C(L, H)$. In terms of dimensionless variables, boundary conditions are taken to be:

1. On the top and bottom of the cylinder $z = 0$ and $z = H$ the normal derivatives satisfy $u_z = v_z = \Theta_z = 0$ together with $w = 0$. This is appropriate for the atmosphere where the heat transport term $q(x, y, t)$ in (2.8) is dominant. Ideally, in the case of the ocean, as in [28, 29], the zero conditions for u_z and v_z on the cylinder top would need to be replaced by a specified wind stress, but this creates surface integrals which can only be estimated in terms of higher derivatives within the cylinder.
2. Periodic boundary conditions on all variables are taken on the side of the cylinder S_C , which is a minor change from those in [28, 29, 33].

The key feature for HPE is the use of enstrophy (i.e. vorticity squared) rather than kinetic energy as a quadratic measure of motion. This means that the pressure gradient is excluded from the dynamics at an early stage and, more importantly, that the analysis is immediately in terms of spatial derivatives of velocity components rather than the components themselves. In contrast, earlier approaches based available potential energy include the pressure field until a global spatial integral removes it and this has made local results more difficult to reach. In addition, energy arguments deliver results about attainable velocities not about velocity gradients.

The vorticity $\zeta = \text{curl } \mathbf{v}$ is specifically given by

$$\zeta = \text{curl } \mathbf{v} = -i v_z + j u_z + \mathbf{k}(v_x - u_y). \quad (2.9)$$

⁶Note that we use the upper-case Θ for the temperature to avoid confusion with lower-case θ which is conventionally used for the potential temperature.

This contains the same \mathbf{k} -component as the full 3D-vorticity $\boldsymbol{\omega} = \nabla_3 \times \mathbf{V}$ but with the w -terms missing. The relation between $\boldsymbol{\zeta}$ and $\boldsymbol{\omega}$ gives rise to a technically important relation

$$-\mathbf{V} \cdot \nabla_3 \mathbf{v} = \mathbf{V} \times \boldsymbol{\zeta} - \frac{1}{2} \nabla_3 (u^2 + v^2). \quad (2.10)$$

Taking the curl of (2.7) gives

$$\varepsilon \frac{\partial \boldsymbol{\zeta}}{\partial t} = \varepsilon Re^{-1} \Delta_3 \boldsymbol{\zeta} + \varepsilon \text{curl}(\mathbf{V} \times \boldsymbol{\zeta}) - \text{curl}(\mathbf{k} \times \mathbf{v} + a_0 \mathbf{k} \Theta). \quad (2.11)$$

This relation forms the basis of the proof of Theorem 1 in §3.

2.2 Non-hydrostatic primitive equations (NPE)

The NPE restore vertical acceleration so that, in contrast to (2.6), the equation for w reads

$$\alpha_a^2 \varepsilon^2 \left(\frac{\partial}{\partial t} + \mathbf{V} \cdot \nabla_3 \right) w + a_0 \Theta + p_z = \varepsilon Re^{-1} \Delta_3 w. \quad (2.12)$$

Using the definition of \mathbf{v} in (2.3) and putting (2.12) together with (2.4) and (2.5) we find

$$\varepsilon \left(\frac{\partial}{\partial t} + \mathbf{V} \cdot \nabla_3 \right) \mathbf{v} + \mathbf{k} \times \mathbf{v} + a_0 \mathbf{k} \Theta = \varepsilon Re^{-1} \Delta_3 \mathbf{v} - \nabla_3 p. \quad (2.13)$$

The equation for the temperature (2.8) remains the same. In contrast to the hydrostatic case where regularity has been established with realistic Neumann-type boundary conditions on the top of a cylinder, several major open questions remain in the non-hydrostatic case:

1. No proof yet exists for the regularity of the NPE (2.13). Their prognostic equation for w brings NPE much closer to the three-dimensional Navier-Stokes equations for a rotating stratified fluid than HPE, in which w is diagnosed from the incompressibility condition. While regularity properties for Navier-Stokes fluids on very thin domains ($0 < \alpha_a \ll 1$) has been established [34, 35], the general regularity problem remains open.
2. The boundary integrals for HPE estimated on the top and bottom of the cylinder $C(H, L)$ are also problematic for NPE. Whereas the vorticity $\boldsymbol{\zeta}$ in the hydrostatic case has only terms u_z and v_z in the horizontal components, which are specified on the top and bottom of $C(H, L)$, the non-hydrostatic vorticity

$$\boldsymbol{\omega} = \text{curl } \mathbf{v} \quad (2.14)$$

also includes w_x and w_y terms which are not specified.

Similar to (2.10), there exists a technical relation between \mathbf{V} , \mathbf{v} and $\boldsymbol{\omega}$

$$-\mathbf{V} \cdot \nabla_3 \mathbf{v} = \mathbf{V} \times \boldsymbol{\omega} - \frac{1}{2} \nabla_3 [u_3^2 - \varepsilon^2 w^2 (\alpha_a^2 - 1)^2], \quad (2.15)$$

so the curl-operation on (2.13) gives

$$\varepsilon \frac{\partial \boldsymbol{\omega}}{\partial t} = \varepsilon Re^{-1} \Delta_3 \boldsymbol{\omega} + \varepsilon \text{curl}(\mathbf{V} \times \boldsymbol{\omega}) - \text{curl}(\mathbf{k} \times \mathbf{v} + a_0 \mathbf{k} \Theta) \quad (2.16)$$

without involving pressure terms.

To address the influence of the material derivative in (2.12), typical values of $\alpha_a^2 \varepsilon^2$ can be determined. Typical observed values for mid-latitude synoptic weather and climate systems are:

$$\begin{aligned}\alpha_a &= H/L \approx 10^4 m / 10^6 m \approx 10^{-2} \\ W/U &\approx 10^{-2} ms^{-1} / 10 ms^{-1} \approx 10^{-3} \\ \varepsilon &= U/(f_0 L) \approx 10 ms^{-1} / (10^{-4} s^{-1} 10^6 m) \approx 10^{-1}.\end{aligned}\tag{2.17}$$

For mid-latitude large-scale ocean circulation, the corresponding numbers are:

$$\begin{aligned}\alpha_a &= H/L \approx 10^3 m / 10^5 m \approx 10^{-2} \\ W/U &\approx 10^{-3} ms^{-1} / 10^{-1} ms^{-1} \approx 10^{-2} \\ \varepsilon &= U/(f_0 L) \approx 10^{-1} ms^{-1} / (10^{-4} s^{-1} 10^5 m) \approx 10^{-2}.\end{aligned}\tag{2.18}$$

Thus, for these typical conditions, $\alpha_a^2 \varepsilon^2 \approx 10^{-8} - 10^{-6} \ll 1$ so the hydrostatic approximation can be expected to be extremely accurate in calculations of either synoptic weather and climate, or large-scale ocean circulation at mid-latitude: see [42, 43, 44].

3 Extreme events & their interpretation

The proof of global existence and uniqueness of solutions of HPE by Cao and Titi guarantees that at each point in space time a unique solution exists [28, 29, 33]. This result can be exploited to prove Theorem 1 and from this to consider the idea of extreme events.

HPE quantity	Definition
Local (horizontal) Reynolds no in terms of $ \mathbf{u} $	$\mathcal{R}_{u_{hor}} = L \mathbf{u} \nu^{-1}$
Local (vertical) Reynolds no in terms of $ u_3 $	$\mathcal{R}_{u_3} = L u_3 \nu^{-1}$
Local Rayleigh no in terms of T	$\mathcal{R}_{a,T} = g\alpha H^3 T (\nu\kappa)^{-1}$
β_1	$\beta_1 = 2L^2 \delta_3 \omega_0^{-2}$
β_2	$\beta_2 = L^4 (1 - 2\delta_3) \sigma^{-1} T_0^{-2}$
$\beta_{u_{hor}}$	$\beta_{u_{hor}} = \frac{9}{4\delta_1^3} + \frac{243}{32\delta_3^3}$
β_{u_3}	$\beta_{u_3} = \left(\frac{3}{2\delta_1^3} + \frac{\sigma^2}{12\delta_3^3} \right)$
$\beta_{1,T}$	$\beta_{1,T} = \frac{\sigma^2}{6} \left(1 + \frac{\sigma}{64} \right) \alpha_a^{-6} \delta_3^{-3}$
$\beta_{2,T}$	$\beta_{2,T} = \frac{\varepsilon^{-2} \alpha_a^{-6}}{2\delta_2}$
\mathcal{V}_*	$\mathcal{V}_* = \pi L^2 H \tau_*$

Table 3: Definitions in the hydrostatic case.

Consider the arbitrary positive constants $0 < \delta_1, \delta_2 < 1$ chosen such that

$$2\delta_3 = 1 - \frac{3}{4}\delta_1 - \delta_2 > 0.\tag{3.1}$$

These are used to define a hydrostatic forcing function $F_H(Q)$:

$$F_H(Q) = \varepsilon^{-2} \left(\delta_2 + \frac{1}{2\delta_2} \right) Re^2 \mathcal{R}_{u_{hor}}^2 + \frac{\sigma}{6\delta_3 T_0^2 \omega_0^2} Re |Q|^2. \quad (3.2)$$

The spatially global quantity $\mathcal{H}(t)$

$$\mathcal{H}(t) = \int_{\mathcal{V}} (Re^3 |\zeta|^2 + Re |\Theta_z|^2) dV. \quad (3.3)$$

is now used in the proof of the following theorem :

Theorem 1 *In $C(H, L)$ over some chosen time interval $[0, \tau_*]$, the space-time 4-integral satisfies*

$$\begin{aligned} \int_0^{\tau_*} \int_{\mathcal{V}} \left\{ -\beta_1 \left[|\nabla_2 \Omega_3|^2 + \alpha_a^2 \left| \frac{\partial^2 u_1}{\partial x_2 \partial x_3} \right|^2 + \alpha_a^2 \left| \frac{\partial^2 u_2}{\partial x_1 \partial x_3} \right|^2 \right] - \beta_2 \alpha_a^2 |\nabla_3 T_{x_3}|^2 + \beta_{u_1} \mathcal{R}_{u_{hor}}^6 \right. \\ \left. + \beta_{u_3} \mathcal{R}_{u_3}^6 + \beta_{1,T} \mathcal{R}_{a,T}^6 + \beta_{2,T} Re^4 \mathcal{R}_{a,T}^2 + F_H(Q) + \frac{1}{2} \mathcal{V}_*^{-1} \mathcal{H}(0) \right\} dx_1 dx_2 dx_3 d\tau > 0 \end{aligned} \quad (3.4)$$

where the coefficients are given in Table 3.

Remark 1: The proof in §3.1 shows that the right hand side of (3.4) is, in fact, $\frac{1}{2} \mathcal{H}(\tau_*)$. Because solutions of HPE are regular this is bounded above for all values of τ_* . However, it has a lower bound of zero which, although not necessarily a good lower bound, is uniform in τ_* . Regularity of solutions is also a necessity in order to extract point-wise functions from within the 4-integral in (3.4).

Remark 2: Of course, any integral of the form $\iint (A - B) dV dt > 0$ trivially indicates that there must be regions of space-time where $A > B$ but, potentially, there could also be regions where $A \leq B$. Such integrals are common, particularly energy integrals, and in most cases the information gained is of little interest. In the case of (3.4), however, the proof in 3.1 will demonstrate that much effort has gone into rigorously manipulating it into a form that produces sensible and recognizable physics. From (3.4) we conclude that :

1. There are regions of space-time $\mathbb{S}^+ \subset \mathbb{R}^4$ on which

$$\begin{aligned} \beta_1 \left[|\nabla_2 \Omega_3|^2 + \alpha_a^2 \left| \frac{\partial^2 u_1}{\partial x_2 \partial x_3} \right|^2 + \alpha_a^2 \left| \frac{\partial^2 u_2}{\partial x_1 \partial x_3} \right|^2 \right] + \beta_2 \alpha_a^2 |\nabla T_{x_3}|^2 \\ < \beta_{u_{hor}} \mathcal{R}_{u_{hor}}^6 + \beta_{u_3} \mathcal{R}_{u_3}^6 + \beta_{1,T} \mathcal{R}_{a,T}^6 + \beta_{2,T} Re^4 \mathcal{R}_{a,T}^2 + F_H(Q) + O(\tau_*^{-1}) \end{aligned} \quad (3.5)$$

2. Potentially there are also regions of space-time $\mathbb{S}^- \subset \mathbb{R}^4$ on which

$$\begin{aligned} \beta_1 \left[|\nabla_2 \Omega_3|^2 + \alpha_a^2 \left| \frac{\partial^2 u_1}{\partial x_2 \partial x_3} \right|^2 + \alpha_a^2 \left| \frac{\partial^2 u_2}{\partial x_1 \partial x_3} \right|^2 \right] + \beta_2 \alpha_a^2 |\nabla T_{x_3}|^2 \\ \geq \beta_{u_{hor}} \mathcal{R}_{u_{hor}}^6 + \beta_{u_3} \mathcal{R}_{u_3}^6 + \beta_{1,T} \mathcal{R}_{a,T}^6 + \beta_{2,T} Re^4 \mathcal{R}_{a,T}^2 + F_H(Q) + O(\tau_*^{-1}) \end{aligned} \quad (3.6)$$

It must be stressed that there is no information here about the nature of the two sets \mathbb{S}^\pm : the 4-integral in (3.4) above yields no more information other than the possibility of a non-empty set \mathbb{S}^- existing. It says nothing about the spatial or temporal statistics of the subsets of \mathbb{S}^- (which

may have a very sensitive τ_* -dependence) nor does it give any indication of their topology. **These results, however, are consistent with the observations of fronts in the atmosphere where large second gradients appear spontaneously in confined spatial regions often disappearing again in an equally spontaneous manner.** This behaviour would also be consistent with \mathbb{S}^- being comprised of a disjoint union of subsets although no details can be deduced from (3.4).

To illustrate the nature of a front, very large values of double mixed-derivatives are required in local parts of the flow as envisaged in the early and pioneering work of Hoskins [23, 24]. For instance, very large values of $|\partial^2 u_1 / \partial x_3 \partial x_2|^2$ or $|\partial^2 u_2 / \partial x_3 \partial x_1|^2$ would represent intense accumulation in the (x_1, x_3) - and (x_2, x_3) -planes respectively.

The large lower bounds in Theorems 1 can be interpreted in terms of a length scale. To achieve this, define the point-wise inverse length scale λ_H^{-1} such that⁷

$$(L\lambda_H^{-1})^6 = L^2\omega_0^{-2} \left(|\nabla_2 \Omega_3|^2 + \alpha_a^2 \left| \frac{\partial^2 u_1}{\partial x_2 \partial x_3} \right|^2 + \alpha_a^2 \left| \frac{\partial^2 u_2}{\partial x_1 \partial x_3} \right|^2 \right) + \alpha_a^2 \beta_2 \beta_1^{-1} L^4 |\nabla_3 T_{x_3}|^2 T_0^{-2}, \quad (3.7)$$

The sixth-powers on the right hand sides of Theorem 1 gives results within \mathbb{S}^-

$$L\lambda_H^{-1} > c_{u_{hor}} \mathcal{R}_{u_{hor}} + c_{u_3} \mathcal{R}_{u_3} + c_{1,T} \mathcal{R}_{a,T} + c_{2,T} Re^{2/3} \mathcal{R}_{a,T}^{1/3} + \text{forcing} \quad (3.8)$$

where the coefficients $c_{u_{hor}}$, c_{u_3} and $c_{i,T}$ can be calculated from Theorems 1: indeed the term \mathcal{R}_{u_3} can be ignored as the vertical velocity $u_3 \sim O(\varepsilon)$. (3.8) can be interpreted as a lower bound on the inverse length scale of the smallest feature in a front. As already noted, no information is available on any statistics nor on the shape and size of subsets of \mathbb{S}^- .

3.1 Proof of Theorem 1

3.1.1 The evolution of the enstrophy

The equation for the HPE enstrophy ζ in (2.11) is now considered on the cylinder $C(H, L)$ with the boundary conditions $u_z = v_z = w = 0$ on the top and bottom but with periodic side-wall conditions

$$\begin{aligned} \frac{1}{2}\varepsilon \frac{d}{dt} \int_{\mathcal{V}} |\zeta|^2 dV &= \varepsilon Re^{-1} \int_{\mathcal{V}} \zeta \cdot \Delta_3 \zeta dV + \varepsilon \int_{\mathcal{V}} \zeta \cdot \text{curl}(\mathbf{V} \times \zeta) dV \\ &\quad - \int_{\mathcal{V}} \zeta \cdot \text{curl}(\mathbf{k} \times \mathbf{v} + a_0 \mathbf{k} \Theta) dV. \end{aligned} \quad (3.9)$$

The notation in the rest of the paper is

$$\|f\|_p = \left(\int_{\mathcal{V}} |f|^p dV \right)^{1/p}. \quad (3.10)$$

Note that in estimating the integrals in (3.9), a standard vector identity and the Divergence Theorem are used in which a surface integral naturally appears each time. However, on the cylinder top and bottom

$$\mathbf{k} \times \zeta = 0 \quad \text{on} \quad z = 0, H. \quad (3.11)$$

⁷The point-wise local length scale λ_H^{-1} is formed in the same dimensional manner as the Kraichnan length ℓ_k , namely, from a combination of the palenstrophy $|\nabla \omega|^2$ and the viscosity ν given by $\ell_k^{-6} = \nu^{-2} |\nabla \omega|^2$.

This and the side-wall periodic boundary conditions make zero all the surface integrals that appear from the Divergence Theorem.

Considering (3.9) term by term, the first is ($\operatorname{div} \zeta = 0$)

$$\int_{\mathcal{V}} \zeta \cdot \Delta_3 \zeta dV = - \int_{\mathcal{V}} \zeta \cdot \operatorname{curl} \operatorname{curl} \zeta dV = - \int_{\mathcal{V}} |\operatorname{curl} \zeta|^2 dV. \quad (3.12)$$

The second integral on the right hand side of (3.9)

$$\int_{\mathcal{V}} \zeta \cdot \operatorname{curl} (\mathbf{V} \times \zeta) dV = \int_{\mathcal{V}} \operatorname{curl} \zeta \cdot (\mathbf{V} \times \zeta) dV, \quad (3.13)$$

and so

$$\left| \int_{\mathcal{V}} \zeta \cdot \operatorname{curl} (\mathbf{V} \times \zeta) dV \right| \leq \|\operatorname{curl} \zeta\|_2 \|\mathbf{V}\|_6 \|\zeta\|_3. \quad (3.14)$$

Thirdly,

$$\int_{\mathcal{V}} \zeta \cdot \operatorname{curl} (\mathbf{k} \times \mathbf{v} + a_0 \mathbf{k} \Theta) dV = \int_{\mathcal{V}} \operatorname{curl} \zeta \cdot (\mathbf{k} \times \mathbf{v} + a_0 \mathbf{k} \Theta) dV. \quad (3.15)$$

Thus (3.9) can be re-written as

$$\begin{aligned} \frac{1}{2} \varepsilon \frac{d}{dt} \int_{\mathcal{V}} |\zeta|^2 dV &\leq -\varepsilon R e^{-1} \int_{\mathcal{V}} |\operatorname{curl} \zeta|^2 dV + \varepsilon \|\operatorname{curl} \zeta\|_2 \|\mathbf{V}\|_6 \|\zeta\|_3 \\ &\quad - \int_{\mathcal{V}} (\operatorname{curl} \zeta) \cdot (\mathbf{k} \times \mathbf{v} + a_0 \mathbf{k} \Theta) dV \\ &\equiv -\varepsilon R e^{-1} \int_{\mathcal{V}} |\operatorname{curl} \zeta|^2 dV + \mathbf{T}1 + \mathbf{T}2 + \mathbf{T}3, \end{aligned} \quad (3.16)$$

where

$$\mathbf{T}1 = \varepsilon \|\operatorname{curl} \zeta\|_2 \|\mathbf{V}\|_6 \|\zeta\|_3 \quad (3.17)$$

$$\mathbf{T}2 = - \int_{\mathcal{V}} (\operatorname{curl} \zeta) \cdot (\mathbf{k} \times \mathbf{v}) dV, \quad \mathbf{T}3 = -a_0 \int_{\mathcal{V}} (\operatorname{curl} \zeta) \cdot (\mathbf{k} \Theta) dV. \quad (3.18)$$

Before estimating $\mathbf{T}1$, $\mathbf{T}2$, and $\mathbf{T}3$, we prove

Lemma 1 *In the cylinder $C(H, L)$*

$$\|\zeta\|_3 \leq 3^{1/2} \|\operatorname{curl} \zeta\|_2^{1/2} \|\mathbf{v}\|_6^{1/2}. \quad (3.19)$$

Proof: Consider

$$\begin{aligned} \int_{\mathcal{V}} |\zeta|^3 dV &= \int_{\mathcal{V}} \zeta \cdot (\zeta \zeta) dV \\ &= \int_{\mathcal{V}} \mathbf{v} \cdot \operatorname{curl} (\zeta \zeta) dV - \int_S \operatorname{div} (\zeta (\mathbf{v} \times \zeta)) dS \\ &= \int_{\mathcal{V}} \mathbf{v} \cdot (\zeta \operatorname{curl} \zeta + (\nabla_3 \zeta) \times \zeta) dV - \int_S \operatorname{div} (\zeta (\mathbf{v} \times \zeta)) dS. \end{aligned} \quad (3.20)$$

The surface integral is zero because $\mathbf{k} \times \zeta = 0$ on the cylinder top and bottom. A vector identity

$$\nabla_3 \zeta = \frac{1}{2} (\zeta)^{-1} \nabla_3 (\zeta \cdot \zeta) = \hat{\zeta} \cdot \nabla_3 \zeta + \hat{\zeta} \times \operatorname{curl} \zeta \quad (3.21)$$

allows us to write

$$\operatorname{curl}(\zeta \zeta) = \zeta \operatorname{curl} \zeta + (\zeta \times \operatorname{curl} \zeta) \times \hat{\zeta} - \zeta \times (\hat{\zeta} \cdot \nabla_3 \zeta), \quad (3.22)$$

so we conclude that

$$\int_{\mathcal{V}} |\zeta|^3 dV = \int_{\mathcal{V}} \mathbf{v} \cdot \left(\zeta \operatorname{curl} \zeta + (\zeta \times \operatorname{curl} \zeta) \times \hat{\zeta} - \zeta \times (\hat{\zeta} \cdot \nabla_3 \zeta) \right) dV. \quad (3.23)$$

Using a Hölder inequality, it is then found that

$$\int_{\mathcal{V}} |\zeta|^3 dV \leq 3 \|\operatorname{curl} \zeta\|_2 \|\zeta\|_3 \|\mathbf{v}\|_6 \quad (3.24)$$

giving the result (3.19). \square

Lemma 2 *Within the cylinder $C(L, H)$, $T1$, $T2$ and $T3$ are estimated as*

$$|T1| \leq \frac{3}{4} \delta_1 \varepsilon Re^{-1} \|\operatorname{curl} \zeta\|_2^2 + \frac{3\varepsilon}{4\delta_1^3} Re^3 (2\|\mathbf{V}\|_6^6 + \|\mathbf{v}\|_6^6) \quad (3.25)$$

for any $\delta_1 > 0$. Moreover, for any $\delta_2 > 0$ and $\delta_2 > 0$

$$|T2| \leq \frac{1}{2} \delta_2 \varepsilon Re^{-1} \|\operatorname{curl} \zeta\|_2^2 + \frac{1}{2} \delta_2^{-1} \varepsilon^{-1} Re \|\mathbf{v}\|_2^2, \quad (3.26)$$

$$|T3| \leq \frac{1}{2} \delta_2 \varepsilon Re^{-1} \|\operatorname{curl} \zeta\|_2^2 + \frac{a_0^2}{2\varepsilon \delta_2} Re \|\Theta\|_2^2. \quad (3.27)$$

Proof: In the following the $\delta_i > 0$ are constants introduced by a series of Young's inequalities:

1) Using Lemma 1 $T1$ can be written as

$$T1 = \varepsilon \|\operatorname{curl} \zeta\|_2 \|\mathbf{V}\|_6 \|\zeta\|_3 \quad (3.28)$$

$$\begin{aligned} &\leq \varepsilon \|\operatorname{curl} \zeta\|_2 \|\mathbf{V}\|_6 \times 3^{1/2} \|\operatorname{curl} \zeta\|_2^{1/2} \|\mathbf{v}\|_6^{1/2} \\ &\leq (\delta_1 \varepsilon Re^{-1} \|\operatorname{curl} \zeta\|_2^2)^{3/4} (9\varepsilon \delta_1^{-3} Re^3 \|\mathbf{V}\|_6^6)^{1/6} (9\varepsilon \delta_1^{-3} Re^3 \|\mathbf{v}\|_6^6)^{1/12} \\ &\leq \frac{3}{4} \delta_1 \varepsilon Re^{-1} \|\operatorname{curl} \zeta\|_2^2 + \frac{3\varepsilon}{4\delta_1^3} Re^3 (2\|\mathbf{V}\|_6^6 + \|\mathbf{v}\|_6^6). \end{aligned} \quad (3.29)$$

2) From (3.18), $T2$ can be estimated as

$$\begin{aligned} |T2| &\leq \|\operatorname{curl} \zeta\|_2 \|\mathbf{v}\|_2 = (\delta_2 \varepsilon Re^{-1} \|\operatorname{curl} \zeta\|_2^2)^{1/2} (\delta_2^{-1} \varepsilon^{-1} Re \|\mathbf{v}\|_2^2)^{1/2} \\ &\leq \frac{1}{2} \delta_2 \varepsilon Re^{-1} \|\operatorname{curl} \zeta\|_2^2 + \frac{1}{2} \delta_2^{-1} \varepsilon^{-1} Re \|\mathbf{v}\|_2^2. \end{aligned} \quad (3.30)$$

3) From (3.18), and using the same constant δ_2 , $T3$ is estimated as

$$\begin{aligned} |T3| &\leq a_0 \|\operatorname{curl} \zeta\|_2 \|\Theta\|_2 = (\delta_2 \varepsilon Re^{-1} \|\operatorname{curl} \zeta\|_2^2)^{1/2} \left(\frac{a_0^2}{\delta_2 \varepsilon} Re \|\Theta\|_2^2 \right)^{1/2} \\ &\leq \frac{1}{2} \delta_2 \varepsilon Re^{-1} \|\operatorname{curl} \zeta\|_2^2 + \frac{a_0^2}{2\delta_2 \varepsilon} Re \|\Theta\|_2^2. \end{aligned} \quad (3.31)$$

as advertized. \square

Returning to (3.9), a division by ε and a gathering terms gives

$$\begin{aligned} \frac{1}{2} \frac{d}{dt} \int_{\mathcal{V}} |\zeta|^2 dV &\leq - (1 - \frac{3}{4} \delta_1 - \delta_2) Re^{-1} \int_{\mathcal{V}} |\text{curl } \zeta|^2 dV \\ &+ \frac{3}{4\delta_1^3} Re^3 (2\varepsilon^6 \|w\|_6^6 + 3\|v\|_6^6) + \frac{1}{\varepsilon^2} \left(\delta_2 + \frac{1}{2\delta_2} \right) Re \|v\|_2^2 + \frac{a_0^2}{2\varepsilon^2 \delta_2} Re \|\Theta\|_2^2. \end{aligned} \quad (3.32)$$

The following Lemma relates $\int_{\mathcal{V}} |\text{curl } \zeta|^2 dV$ to sums of squares.

Lemma 3 *Let ω_3 be the third component of the full vorticity $\omega = \nabla_3 \times \mathbf{V} = (\omega_1, \omega_2, \omega_3)$. Then for any $0 < \delta_0 < 1$*

$$\begin{aligned} \int_{\mathcal{V}} |\text{curl } \zeta|^2 dV &> \min\{1, 2(1 - \delta_0)\} \int_{\mathcal{V}} |\nabla_2 \omega_3|^2 dV + 2\delta_0 \int_{\mathcal{V}} \{|u_{yz}|^2 + |v_{xz}|^2\} dV \\ &+ \int_{\mathcal{V}} \{|u_{zz}|^2 + |v_{zz}|^2 + \varepsilon^2(1 - \delta_0)|w_{zz}|^2\} dV. \end{aligned} \quad (3.33)$$

Proof: Using ζ in (2.9) in the form $\zeta = -v_z \mathbf{i} + u_z \mathbf{j} + \omega_3 \mathbf{k}$ with $\omega_3 = v_x - u_y$ and recalling that $\varepsilon w_z = -(u_x + v_y)$

$$\text{curl } \zeta = \begin{vmatrix} \mathbf{i} & \mathbf{j} & \mathbf{k} \\ \partial_x & \partial_y & \partial_z \\ -v_z & u_z & \omega_3 \end{vmatrix} = \mathbf{i}(\omega_{3,y} - u_{zz}) - \mathbf{j}(\omega_{3,x} + v_{zz}) - \varepsilon \mathbf{k} w_{zz} \quad (3.34)$$

Thus

$$|\text{curl } \zeta|^2 = |\nabla_2 \omega_3|^2 + (u_{zz}^2 + v_{zz}^2 + \varepsilon^2 w_{zz}^2) - 2(\omega_{3,y} u_{zz} - \omega_{3,x} v_{zz}). \quad (3.35)$$

Now, invoking the boundary conditions and the fact that $\omega_3 = v_x - u_y$, integration by parts gives

$$- 2 \int_{\mathcal{V}} (\omega_{3,y} u_{zz} - \omega_{3,x} v_{zz}) dV = 2 \int_{\mathcal{V}} |\omega_{3,z}|^2 dV \quad (3.36)$$

and so

$$\int_{\mathcal{V}} |\text{curl } \zeta|^2 dV = \int_{\mathcal{V}} \{|\nabla_2 \omega_3|^2 + 2|\omega_{3,z}|^2 dV\} + \int_{\mathcal{V}} \{u_{zz}^2 + v_{zz}^2 + \varepsilon^2 w_{zz}^2\} dV. \quad (3.37)$$

Moreover, it is easily shown that

$$\begin{aligned} \int_{\mathcal{V}} (\varepsilon^2 |w_{zz}|^2 + 2|\omega_{3,z}|^2) dV &= \int_{\mathcal{V}} \{(u_{xz} - v_{yz})^2 + 2(u_{yz}^2 + v_{xz}^2)\} dV \\ &> 2 \int_{\mathcal{V}} (u_{yz}^2 + v_{xz}^2) dV \end{aligned} \quad (3.38)$$

where a pair of horizontal integrations by parts in the first line of (3.38) have been performed. A linear combination of (3.37) and (3.38) gives

$$\begin{aligned} \int_{\mathcal{V}} |\text{curl } \zeta|^2 dV &= \int_{\mathcal{V}} \{|\nabla_2 \omega_3|^2 + 2|\omega_{3,z}|^2 dV\} + \int_{\mathcal{V}} \{u_{zz}^2 + v_{zz}^2 + \varepsilon^2 w_{zz}^2\} dV \\ &> \int_{\mathcal{V}} \{|\nabla_2 \omega_3|^2 + 2(1 - \delta_0)|\omega_{3,z}|^2 dV\} \\ &+ \int_{\mathcal{V}} \{u_{zz}^2 + v_{zz}^2 + (1 - \delta_0)\varepsilon^2 w_{zz}^2\} dV + 2\delta_0 \int_{\mathcal{V}} (u_{yz}^2 + v_{xz}^2) dV, \end{aligned} \quad (3.39)$$

which gives (3.33). This completes the proof. \square

3.1.2 The evolution of $\int_{\mathcal{V}} |\Theta_z|^2 dV$

The partial differential equation for Θ given in (2.8) with BCs applied on $C(L, H)$

$$\frac{\partial \Theta}{\partial t} + \mathbf{V} \cdot \nabla_3 \Theta = (\sigma Re)^{-1} \Delta_3 \Theta + q \quad (3.40)$$

is now differentiated with respect to z to give

$$\begin{aligned} \frac{1}{2} \frac{d}{dt} \int_{\mathcal{V}} |\Theta_z|^2 dV &= (\sigma Re)^{-1} \int_{\mathcal{V}} \Theta_z (\Delta_3 \Theta_z) dV - \int_{\mathcal{V}} \Theta_z \frac{\partial}{\partial z} (\mathbf{V} \cdot \nabla_3 \Theta) dV + \int_{\mathcal{V}} \Theta_z q_z dV \\ &= -(\sigma Re)^{-1} \int_{\mathcal{V}} |\nabla_3 \Theta_z|^2 dV - \int_{\mathcal{V}} \mathbf{V} \cdot \nabla_3 (\tfrac{1}{2} \Theta_z^2) dV \\ &\quad - \int_{\mathcal{V}} \Theta_z (u_z \Theta_x + v_z \Theta_y + \varepsilon w_z \Theta_z) dV + \int_{\mathcal{V}} \Theta_z q_z dV. \end{aligned} \quad (3.41)$$

However, given that $\operatorname{div} \mathbf{V} = 0$ and $w = 0$ on S^\pm

$$\begin{aligned} \int_{\mathcal{V}} \mathbf{V} \cdot \nabla_3 (\tfrac{1}{2} \Theta_z^2) dV &= \int_{\mathcal{V}} \{ \operatorname{div} (\tfrac{1}{2} \Theta_z^2 \mathbf{V}) - \tfrac{1}{2} \Theta_z^2 \operatorname{div} \mathbf{V} \} dV \\ &= \tfrac{1}{2} \int_S (\hat{\mathbf{n}} \cdot \mathbf{V}) \Theta_z^2 dS \\ &= \pm \tfrac{1}{2} \varepsilon \int_{S^\pm} w \Theta_z^2 dx dy = 0. \end{aligned} \quad (3.42)$$

Integrating by parts the 3rd and 4th terms in (3.41) gives

$$\begin{aligned} \frac{1}{2} \frac{d}{dt} \int_{\mathcal{V}} |\Theta_z|^2 dV &= -(\sigma Re)^{-1} \int_{\mathcal{V}} |\nabla_3 \Theta_z|^2 dV + \int_{\mathcal{V}} \Theta_z (u_{xz} + v_{yz} + \varepsilon w_{zz}) \Theta dV \\ &\quad + \int_{\mathcal{V}} \Theta (u_z \Theta_{xz} + v_z \Theta_{yz} + \varepsilon w_z \Theta_{zz}) dV - \int_{\mathcal{V}} \Theta_{zz} q dV \\ &= -(\sigma Re)^{-1} \int_{\mathcal{V}} |\nabla_3 \Theta_z|^2 dV + \int_{\mathcal{V}} \Theta (u_z \Theta_{xz} + v_z \Theta_{yz} + \varepsilon w_z \Theta_{zz}) dV \\ &\quad - \int_{\mathcal{V}} \Theta_{zz} q dV \end{aligned} \quad (3.43)$$

where $\operatorname{div} \mathbf{V} = 0$ has been used. Using a Hölder inequality it is found that

$$\begin{aligned} \frac{1}{2} \frac{d}{dt} \int_{\mathcal{V}} |\Theta_z|^2 dV &\leq -(\sigma Re)^{-1} \int_{\mathcal{V}} |\nabla_3 \Theta_z|^2 dV + \|\Theta_{zz}\|_2 \|q\|_2 \\ &\quad + \|\Theta\|_6 \{ \|u_z\|_3 \|\Theta_{xz}\|_2 + \|v_z\|_3 \|\Theta_{yz}\|_2 + \varepsilon \|w_z\|_3 \|\Theta_{zz}\|_2 \}. \end{aligned} \quad (3.44)$$

The next task, addressed in the following Lemma, is to estimate $\|u_z\|_3$, $\|v_z\|_3$ and $\|w_z\|_3$ in terms of their second derivatives.

Lemma 4 *With Neumann boundary conditions on $C(H, L)$, the vector \mathbf{v}_z and the scalar w_z satisfy*

$$\|\mathbf{v}_z\|_3 \leq 6^{1/2} \|\mathbf{v}_{zz}\|_2^{1/2} \|\mathbf{v}\|_6^{1/2}, \quad (3.45)$$

$$\|w_z\|_3 \leq 2^{1/2} \|w_{zz}\|_2^{1/2} \|w\|_6^{1/2}. \quad (3.46)$$

Proof:

$$\begin{aligned} \int_{\mathcal{V}} |\mathbf{v}_z|^3 dV &= \int_{\mathcal{V}} (|u_z|^2 + |v_z|^2)^{3/2} dV \\ &\leq \frac{3}{2} \int_{\mathcal{V}} (|u_z|^3 + |v_z|^3) dV \end{aligned} \quad (3.47)$$

and, given the boundary conditions on u and v ,

$$\begin{aligned} \int_{\mathcal{V}} |u_z|^3 dV &= \int_{\mathcal{V}} u_z u_z |u_z| dV \\ &= - \int_{\mathcal{V}} \left\{ u u_{zz} |u_z| + u u_z \frac{d|u_z|}{dz} \right\} dV + \int_{S^\pm} u u_z |u_z| dx dy \\ &\leq 2 \int_{\mathcal{V}} |u| |u_{zz}| |u_z| dV. \end{aligned} \quad (3.48)$$

which holds because $d|f|/dz \leq |f_z|$ for any appropriately function differentiable f . Thus (3.47) becomes

$$\begin{aligned} \int_{\mathcal{V}} |\mathbf{v}_z|^3 dV &\leq 3 \int_{\mathcal{V}} \{ |u| |u_{zz}| |u_z| + |v| |v_{zz}| |v_z| \} dV \\ &\leq 6 \int_{\mathcal{V}} |\mathbf{v}| |\mathbf{v}_{zz}| |\mathbf{v}_z| dV \\ &\leq 6 \|\mathbf{v}\|_6 \|\mathbf{v}_{zz}\|_2 \|\mathbf{v}_z\|_3, \end{aligned} \quad (3.49)$$

which gives the advertised result. The result for w follows in a similar manner. \square

Continuing with (3.44), multiplying by Re^γ , where γ is to be determined, (3.44) becomes

$$\begin{aligned} \frac{1}{2} \frac{d}{dt} Re^\gamma \int_{\mathcal{V}} |\Theta_z|^2 dV &\leq -(\sigma Re)^{-1} Re^\gamma \int_{\mathcal{V}} |\nabla_3 \Theta_z|^2 dV + 2^{1/2} \varepsilon Re^\gamma \|\Theta\|_6 \|w\|_6^{1/2} \|w_{zz}\|_2^{1/2} \|\Theta_{zz}\|_2 \\ &\quad + 6^{1/2} Re^\gamma \|\mathbf{v}_{zz}\|_2^{1/2} \|\mathbf{v}\|_6^{1/2} \|\Theta\|_6 \{ \|\Theta_{xz}\|_2 + \|\Theta_{yz}\|_2 \} \\ &\quad + Re^\gamma \|\Theta_{zz}\|_2 \|q\|_2. \end{aligned} \quad (3.50)$$

In turn, this re-arranges to

$$\begin{aligned} \frac{1}{2} Re^\gamma \frac{d}{dt} \int_{\mathcal{V}} |\Theta_z|^2 dV &\leq -(\sigma Re)^{-1} Re^\gamma \int_{\mathcal{V}} |\nabla_3 \Theta_z|^2 dV \\ &\quad + \left[4\delta_3 Re^{-1} \varepsilon^2 \|w_{zz}\|_2^2 \right]^{1/4} \left[\delta_3 (\sigma Re)^{-1} Re^\gamma \|\Theta_{zz}\|_2^2 \right]^{1/2} \\ &\quad \times \left[\delta_3^{-3} \sigma^2 Re^{b_1} \|\Theta\|_6^6 \right]^{1/6} \left[\delta_3^{-3} \varepsilon^6 \sigma^2 Re^{b_2} \|w\|_6^6 \right]^{1/12} \\ &\quad + \left\{ \left[4\delta_4 Re^{-1} \|\mathbf{v}_{zz}\|_2^2 \right]^{1/4} \left[3^6 \delta_4^{-3} Re^{c_2} \|\mathbf{v}\|_6^6 \right]^{1/12} \right\} \\ &\quad \times \left[\frac{\sigma^3}{8\delta_4^3} Re^{c_1} \|\Theta\|_6^6 \right]^{1/6} \left\{ 2\delta_4 (\sigma Re)^{-1} Re^\gamma [\|\Theta_{xz}\|_2^2 + \|\Theta_{yz}\|_2^2] \right\}^{1/2} \\ &\quad + \left\{ \delta_5 (\sigma Re)^{-1} Re^\gamma \|\Theta_{zz}\|_2^2 \right\}^{1/2} \left\{ \delta_5^{-1} (\sigma Re) Re^\gamma \|q\|_2^2 \right\}^{1/2}. \end{aligned} \quad (3.51)$$

where $2b_1 + b_2 = 9 + 6\gamma$ and $2c_1 + c_2 = 9 + 6\gamma$. Using Young's inequality it is found that

$$\begin{aligned}
\frac{1}{2}Re^\gamma \frac{d}{dt} \int_{\mathcal{V}} |\Theta_z|^2 dV &\leq -(\sigma Re)^{-1} Re^\gamma \int_{\mathcal{V}} |\nabla_3 \Theta_z|^2 dV \\
&+ \delta_3 Re^{-1} \varepsilon^2 \|w_{zz}\|_2^2 + \frac{1}{2} \delta_3 (\sigma Re)^{-1} Re^\gamma \|\Theta_{zz}\|_2^2 \\
&+ \frac{1}{6} \delta_3^{-3} \sigma^2 Re^{b_1} \|\Theta\|_6^6 + \frac{1}{12} \delta_3^{-3} \varepsilon^6 \sigma^2 Re^{b_2} \|w\|_6^6 \\
&+ \delta_4 Re^{-1} \|\mathbf{v}_{zz}\|_2^2 + \delta_4 (\sigma Re)^{-1} Re^\gamma [\|\Theta_{xz}\|_2^2 + \|\Theta_{yz}\|_2^2] \\
&+ \frac{1}{48 \delta_4^3} \sigma^3 Re^{c_1} \|\Theta\|_6^6 + \frac{3^6}{12 \delta_4^3} Re^{c_2} \|\mathbf{v}\|_6^6 \\
&+ \frac{1}{2} \delta_5 (\sigma Re)^{-1} Re^\gamma \|\Theta_{zz}\|_2^2 + \frac{1}{2} \delta_5^{-1} (\sigma Re) Re^\gamma \|q\|_2^2
\end{aligned} \tag{3.52}$$

Gathering terms we find

$$\begin{aligned}
\frac{1}{2}Re^\gamma \frac{d}{dt} \int_{\mathcal{V}} |\Theta_z|^2 dV &\leq -(\sigma Re)^{-1} Re^\gamma \int_{\mathcal{V}} \left\{ (1 - \delta_4) (|\Theta_{xz}|^2 + |\Theta_{yz}|^2) + (1 - \frac{1}{2} \delta_3 - \frac{1}{2} \delta_5) |\Theta_{zz}|^2 \right\} dV \\
&+ Re^{-1} \left\{ \delta_4 \|\mathbf{v}_{zz}\|_2^2 + \delta_3 \varepsilon^2 \|w_{zz}\|_2^2 \right\} + \frac{3^6}{12 \delta_4^3} Re^{c_2} \|\mathbf{v}\|_6^6 \\
&+ \left\{ \frac{\sigma^2}{6 \delta_3^3} Re^{b_1} + \frac{\sigma^3}{48 \delta_4^3} Re^{c_1} \right\} \|\Theta\|_6^6 + \frac{\varepsilon^6 \sigma^2}{12 \delta_3^3} Re^{b_2} \|w\|_6^6 \\
&+ \frac{1}{2} \delta_5^{-1} (\sigma Re) Re^\gamma \|q\|_2^2.
\end{aligned} \tag{3.53}$$

3.1.3 A combination of the fluid and temperature inequalities

(3.53) is now combined with (3.32)

$$\begin{aligned}
\frac{d}{dt} \int_{\mathcal{V}} |\zeta|^2 dV &+ \frac{1}{2} Re^\gamma \frac{d}{dt} \int_{\mathcal{V}} |\Theta_z|^2 dV \\
&\leq - (1 - \frac{3}{4} \delta_1 - \delta_2) Re^{-1} \int_{\mathcal{V}} |\text{curl } \zeta|^2 dV \\
&- (\sigma Re)^{-1} Re^\gamma \int_{\mathcal{V}} \left\{ (1 - \delta_4) (|\Theta_{xz}|^2 + |\Theta_{yz}|^2) + (1 - \frac{1}{2} \delta_3 - \frac{1}{2} \delta_5) |\Theta_{zz}|^2 \right\} dV \\
&+ Re^{-1} \left\{ \delta_4 \|\mathbf{v}_{zz}\|_2^2 + \delta_3 \varepsilon^2 \|w_{zz}\|_2^2 \right\} + \left(\frac{9}{4 \delta_1^3} Re^3 + \frac{3^6}{12 \delta_4^3} Re^{c_2} \right) \|\mathbf{v}\|_6^6 \\
&+ \varepsilon^6 \left(\frac{3}{2 \delta_1^3} Re^3 + \frac{\sigma^2}{12 \delta_3^3} Re^{b_2} \right) \|w\|_6^6 + \left(\frac{\sigma^2}{6 \delta_3^3} Re^{b_1} + \frac{\sigma^3}{48 \delta_4^3} Re^{c_1} \right) \|\Theta\|_6^6 \\
&+ \frac{1}{\varepsilon^2} \left(\delta_2 + \frac{1}{2 \delta_2} \right) Re \|\mathbf{v}\|_2^2 + \frac{a_0^2}{2 \varepsilon^2 \delta_2} Re \|\Theta\|_2^2 + \frac{1}{2} \delta_5^{-1} (\sigma Re) Re^\gamma \|q\|_2^2
\end{aligned} \tag{3.54}$$

and

$$\left. \begin{aligned} 2b_1 + b_2 \\ 2c_1 + c_2 \end{aligned} \right\} = 9 + 6\gamma \tag{3.55}$$

Our choices are

$$b_1 = c_1 = -3, \quad b_2 = c_2 = 3, \quad \gamma = -2. \tag{3.56}$$

δ_3 and δ_4 also need to be chosen such that the $\|\mathbf{v}_{zz}\|^2$ - and $\varepsilon^2\|w_{zz}\|^2$ -terms cancel from $\|\text{curl } \boldsymbol{\zeta}\|_2^2$. To this end we choose $\delta_0 = \frac{1}{2}$ and make

$$\begin{aligned} 1 - \frac{3}{4}\delta_1 - \delta_2 &= \delta_4 \\ (1 - \frac{3}{4}\delta_1 - \delta_2)(1 - \delta_0) &= \delta_3. \end{aligned} \quad (3.57)$$

Hence $\delta_4 = 2\delta_3$. With this we choose δ_5 such that the coefficients $1 - \delta_4$ and $1 - \frac{1}{2}\delta_3 - \frac{1}{2}\delta_5$ within the double derivatives of the temperature are equal. Thus $\delta_5 = 3\delta_3$. Together we have

$$\delta_3 = \frac{1}{2}(1 - \frac{3}{4}\delta_1 - \delta_2), \quad \delta_4 = 2\delta_3, \quad \delta_5 = 3\delta_3. \quad (3.58)$$

where $\delta_1 > 0$ and $\delta_2 > 0$ are arbitrarily chosen under the constraint that $\delta_3 > 0$.

Now we turn to the last three steps in the calculation :

Step 1 : To deal with the first set of terms on the right hand side of (3.54) we use the expression for $\|\text{curl } \boldsymbol{\zeta}\|_2^2$ in Lemma 3 with $\delta_0 = \frac{1}{2}$ and write

$$\int_{\mathcal{V}} |\text{curl } \boldsymbol{\zeta}|^2 dV - \left(\|\mathbf{v}_{zz}\|_2^2 + \frac{1}{2}\varepsilon^2\|w_{zz}\|_2^2 \right) > \int_{\mathcal{V}} \{ |\nabla_2 \omega_3|^2 + |u_{yz}|^2 + |v_{xz}|^2 \} dV \quad (3.59)$$

This turns (3.54) into

$$\begin{aligned} \frac{1}{2} \frac{d}{dt} \int_{\mathcal{V}} |\boldsymbol{\zeta}|^2 dV &+ \frac{1}{2} Re^{-2} \frac{d}{dt} \int_{\mathcal{V}} |\Theta_z|^2 dV \\ &\leq -2\delta_3 Re^{-1} \int_{\mathcal{V}} \{ |\nabla_2 \omega_3|^2 + |u_{yz}|^2 + |v_{xz}|^2 \} dV \\ &- \sigma^{-1}(1 - 2\delta_3) Re^{-3} \int_{\mathcal{V}} |\nabla_3 \Theta_z|^2 dV + \left(\frac{9}{4\delta_1^3} + \frac{243}{32\delta_3^3} \right) Re^3 \|\mathbf{v}\|_6^6 \\ &+ \varepsilon^6 \left(\frac{3}{2\delta_1^3} + \frac{\sigma^2}{12\delta_3^3} \right) Re^3 \|w\|_6^6 + \frac{\sigma^2}{6\delta_3^3} \left(1 + \frac{\sigma}{64} \right) Re^{-3} \|\Theta\|_6^6 \\ &+ \varepsilon^{-2} Re \left[\left(\delta_2 + \frac{1}{2\delta_2} \right) \|\mathbf{v}\|_2^2 + \frac{a_0^2}{2\delta_2} \|\Theta\|_2^2 \right] + \frac{\sigma}{6\delta_3} Re^{-1} \|q\|_2^2. \end{aligned} \quad (3.61)$$

Step 2 : Now this inequality is re-scaled back to dimensional variables defined in Table 2 and $\mathcal{H}(t)$ defined in (3.3). This involves multiplying both sides of (3.60) by Re^3 .

$$\begin{aligned} \frac{1}{2} \frac{d\mathcal{H}}{dt} &\leq -\frac{2\delta_3 L^2}{\omega_0^2} \int_{\mathcal{V}} (|\nabla_2 \Omega_3|^2 + \alpha_a^2 |u_{1,x_2 x_3}|^2 + \alpha_a^2 |u_{2,x_1 x_3}|^2) dV - \frac{(1 - 2\delta_3)L^4}{\sigma T_0^2} \int_{\mathcal{V}} |\nabla T_{x_3}|^2 dV \\ &+ \left(\frac{9}{4\delta_1^3} + \frac{243}{32\delta_3^3} \right) \|\mathcal{R}_{u_{hor}}\|_6^6 + \left(\frac{3}{2\delta_1^3} + \frac{\sigma^2}{12\delta_3^3} \right) \|\mathcal{R}_{u_3}\|_6^6 + \frac{\alpha_a^{-6} \sigma^2}{6\delta_3^3} \left(1 + \frac{\sigma}{64} \right) \|\mathcal{R}_{a,T}\|_6^6 \\ &+ \varepsilon^{-2} \left\{ \left(\delta_2 + \frac{1}{2\delta_2} \right) Re^2 \|\mathcal{R}_{u_1}\|_2^2 + \frac{a_0^2 \alpha_a^{-6}}{2\delta_2} Re^4 \|\mathcal{R}_{a,T}\|_2^2 \right\} + \frac{\sigma}{6\delta_3} Re \|q\|_2^2. \end{aligned} \quad (3.62)$$

Step 3 : Finally, we take the time integral over an interval $[0, \tau_*]$.

$$\begin{aligned} \int_0^{\tau_*} \int_{\mathcal{V}} \{ &-\frac{2\delta_3 L^2}{\omega_0^2} \{ |\nabla_2 \Omega_3|^2 + \alpha_a^2 |u_{1,x_2 x_3}|^2 + \alpha_a^2 |u_{2,x_1 x_3}|^2 \} - \frac{(1 - 2\delta_3)L^4}{\sigma T_0^2} |\nabla T_{x_3}|^2 \\ &+ \beta_{u_{hor}} |\mathcal{R}_{u_{hor}}|^6 + \beta_{u_3} |\mathcal{R}_{u_3}|^6 + \beta_{1,T} |\mathcal{R}_{a,T}|^6 + \beta_{2,T} Re^4 \mathcal{R}_{a,T}^2 + F_H(Q) \\ &+ \frac{1}{2} \mathcal{V}_*^{-1} \mathcal{H}(0) \} dV dt \geq \frac{1}{2} \mathcal{H}(\tau_*). \end{aligned} \quad (3.63)$$

Because of regularity [28, 29, 30, 31] $\mathcal{H}(\tau_*)$ is always under control from above and it also has a uniform lower bound $\mathcal{H}(\tau_*) > 0$ although zero may be a poor lower bound.

Together with the use of Lemma 3 with $\delta_0 = \frac{1}{2}$, gives the result of Theorem 1, where $\beta_{u_{hor}}$, β_{u_3} and $\beta_{i,T}$ are defined in Table 3 and the forcing function $F_H(Q)$ is defined in (3.2). ■

4 Potential implications for simulations

The main result of this paper is that solutions of HPE can potentially develop extremely small scales of motion, allowed by the estimates derived here. These size scales decrease as \mathcal{R}_u^{-1} and $\mathcal{R}_{a,T}^{-1}$, which means they could easily become of the order of metres or less at the very large values of these parameters achieved in both atmospheric and oceanic flows. The hydrostatic estimate for the length scale defined λ_H in (3.7) is of the order of a *metre* or less. Of course, this very small estimate may not be the thickness of a front; instead, it may refer to the smallest scale of features *within* a front. The importance of the tendency to produce vigorous intermittent small scales in NWP and ocean circulation simulations remains to be determined but it may effect parameterizations as numerical resolution improves. In particular, one may ask whether parameterizations developed at coarser scales will still be accurate at finer scales, if the finer scales undergo the extreme events whose potential appearance has been predicted in this paper. As for the perennial question of initial conditions, one must hope that flow activity initialized at coarse scales will be consistently followed to smaller scales without undue amplification of simulation errors.

The consequences of Theorem 1 in §3 is that space-time is potentially divided into two regions \mathbb{S}^+ and \mathbb{S}^- . The region \mathbb{S}^- could be a union of a large number of disjoint sets, and if it were non-empty the flows in \mathbb{S}^- would be dominated by strong concentrated structures. Very large lower bounds on double mixed derivatives of components of the velocity field (u_1, u_2, u_3) such as $|\partial^2 u_1 / \partial x_3 \partial x_2|^2$ or $|\partial^2 u_2 / \partial x_1 \partial x_3|^2$ may occur within \mathbb{S}^- , thus representing intense accumulation in the (x_1, x_3) - and (x_2, x_3) -planes respectively. For a nonempty \mathbb{S}^- , one would see the spontaneously formation of front-like objects localised in space that would only exist for a finite time. $\mathcal{R}_{u_{hor}}$ is a *local* horizontal Reynolds number depending upon the local space-time values of $u(x_1, x_2, x_3, \tau) = \sqrt{u_1^2 + u_2^2}$ and $\mathcal{R}_{a,T}$ is a Rayleigh number dependent on the local temperature $T(x_1, x_2, x_3, \tau)$. The large lower bounds on double-derivatives of solutions within the \mathbb{S}^- regions can be converted into the large lower bounds on inverse length scales λ_H^{-1} . Thus to resolve a region such as this would require⁸

$$\text{Number of grid points} > \text{const} (\mathcal{R}_{u_{hor}}^3 + \mathcal{R}_{a,T}^3 + Re^2 \mathcal{R}_{a,T}). \quad (4.1)$$

It is also worth remarking that the L^6 -norm arising in the proof of Theorem 3.1, leading to the sixth powers of the *local* Reynolds numbers $\mathcal{R}_{u_{hor}}$ for λ_H^{-1} , is precisely the norm that was proved by Cao and Titi [28, 29] to be bounded for HPE. While $\mathcal{R}_{u_{hor}}$ is a function of space-time it is a bounded function, but how much $\mathcal{R}_{u_{hor}}$ oscillates around its global space-time average Re is unknown: this could vary significantly in different parts of the flow. Thus, how $\mathbf{u}_3 = \{u_1, u_2, u_3\}$ varies across a front is an important issue. The limitations of the result are that no further information is available from the analysis regarding the spatial or temporal statistics of the subsets of \mathbb{S}^- on which intense events would occur.

⁸ \mathcal{R}_{u_3} is expected to be negligible compared to $\mathcal{R}_{u_{hor}}$ because $u_3 \sim O(\varepsilon)$.

If the regularity problem were to be settled in the NPE case, the results would likely be qualitatively the same but with a non-negligible \mathcal{R}_{u_3} term whose contribution may be significant in regions of strong vertical convection. There would also have to be significant technical differences: the domain would need to be made periodic in the velocity variables and their derivatives because of lack of specification of horizontal velocity derivatives.

Future improvements in numerical capabilities for the prediction of weather, climate and ocean circulation may be expected to enhance spatial and temporal resolutions. In addition, they will raise the issue of the optimal allocation of numerical resources. For example, improving the computations for parameterizations of other currently unresolved physical processes (such as phase changes in cloud physics) may have effects that are at least as significant as computing non-hydrostatic effects at finer resolution. Improvements in resolution will also raise the issue of whether subgrid-scale parameterizations of these unresolved physical processes that have been developed for numerical prediction at coarser scales will transfer accurately to computations at finer scales, regardless of whether the hydrostatic approximation is retained. Thus, one may expect the HPE to remain central in the discussions about choices among the various potential numerical code implementations for weather, climate and ocean circulation predictions well into the foreseeable future. Even though they are mathematically well-posed, the HPE have been shown here to contain the potential for sudden, localized events to occur on extremely small scales in space and time.

Acknowledgements : We thank Peter Bartello, Raymond Hide, Brian Hoskins, Tim Palmer & Edriss Titi for several enlightening conversations. Darryl Holm thanks the Royal Society for a Wolfson Research Merit Award.

References

- [1] Richardson, L. F. 1922 *Weather Prediction by Numerical Process* (Cambridge: Cambridge University Press) reprinted 1988 by New York: Dover.
- [2] Charney, J. G. 1955 The use of the primitive equations of motion in numerical prediction, *Tellus*, **7**, 22–26.
- [3] Eckart, C. 1960 *The Hydrodynamics of Oceans and Atmospheres*, Oxford: Pergamon Press.
- [4] Gill, A. 1982 *Atmosphere-ocean dynamics*, London: Academic Press.
- [5] Pedlosky, J. 1987 *Geophysical Fluid Dynamics*, 2nd edition New York: Springer-Verlag.
- [6] Salmon, R. 1988 Hamiltonian fluid mechanics *Ann. Rev. Fluid Mech.*, **20**, 225–256.
- [7] Holton, J. R. 1992 *An Introduction to Dynamic Meteorology* 3rd edition, San Diego: Academic Press.
- [8] Cullen, M. J. P. 1993 The unified forecast/climate model, *Meteorol. Mag.*, **122**, 81–94.
- [9] Holm, D. D. 1996 Hamiltonian balance equations, *Physica D*, **98**, 379–414.
- [10] Marshall, J., Hill, C., Perelman, L. and Adcroft, A. 1997 Hydrostatic, quasi-hydrostatic and non-hydrostatic ocean modelling, *J. Geophys. Res.*, **102**, 5733–5752.
- [11] Norbury, J. and Roulstone, I. 2002 *Large-scale atmosphere-ocean dynamics I & II*, Cambridge: Cambridge University Press.
- [12] White, A. A. 2002 A view of the equations of meteorological dynamics and various approximations, in Norbury, J. and Roulstone, I. (eds) *Large-scale ocean-atmosphere dynamics I*, Cambridge: University Press.
- [13] White, A. A. 2003 Primitive Equations in Holton J. R. et al (eds) *Encyclopedia of atmospheric science* pp 694–702, New York: Academic Press.

- [14] Davies, T., Cullen, M. J. P., Malcolm, A. J., Mawson M., H., Staniforth, A., White, A. A. and Wood N. 2005 A new dynamical core for the Met Office's global and regional modelling of the atmosphere, *J. R. Met. Soc.* **131**, 1759–1782.
- [15] White, A. A., Hoskins, B. J., Roulstone, I. and Staniforth, A. 2005 Consistent approximate models of the global atmosphere: shallow, deep, hydrostatic, quasi-hydrostatic and non-hydrostatic, *Quart. J. R. Met. Soc.* **131**, 2081–2107.
- [16] Cullen, M. J. P. 2006 *A Mathematical Theory of Large-scale Atmosphere/Ocean Flow*, London: Imperial College Press.
- [17] Cullen, M. J. P. 2007 Modelling Atmospheric Flows, *Acta Numerica*, 1–87.
- [18] Wedi, N. P. and Smolarkiewicz, P. K. 2009 A framework for testing global non-hydrostatic models, *Q. J. R. Meteorol. Soc.* (Published online:DOI: 10.1002/qj)
- [19] Ohfuchi, W., Sasaki, H., Masumoto, Y. and Nakamura, H. 2005 Mesoscale resolving simulations of the global atmosphere and ocean on the Earth Simulator *EOS Trans. AGU*, **86**, 45–46.
- [20] Shen, B.-W., Atlas, R., Chern, J.-D., Reale, O., Lin, S.-J., Lee, T. and Chang, J. 2006 The 0.125 degree finite-volume general circulation model on the NASA Columbia supercomputer: preliminary simulations of mesoscale vortices, *Geophys. Res. Lett.*, **33**, L05801.
- [21] Hamilton, K., Takahashi Y. O., and Ohfuchi, W. 2008 The mesoscale spectrum of atmospheric motions investigated in a very fine resolution global general circulation model, *J. Geophys. Res.*, **113**, D18110. doi:10.1029/2008JD009785
- [22] Eliassen, A. 1948 The quasi-static equations of motion, *Geofys Publikasjoner*, **17**, No. 3.
- [23] Hoskins, B. J. 1975 The Geostrophic momentum approximation and the semi-geostrophic equations, *J. Atmos. Sci.*, **32**, 233–242.
- [24] Hoskins, B. J. 1982 The mathematical theory of frontogenesis, *Ann. Rev. Fluid Mech.* **14**, 131–151.
- [25] Hoskins, B. J. and Bretherton, F. 1972 Atmospheric frontogenesis models; Mathematical formulation and solution, *J. Atmos. Sci.*, **29**, 11–37.
- [26] Shapiro, M. A. 1984 Meteorological tower measurements of a surface cold front *Mon. Weather Rev.*, **112**, 1634–1639.
- [27] Weaver, J. F. and Purdom, J. F. W. 1995 An Interesting Mesoscale Storm-Environment Interaction Observed Just Prior to Changes in Severe Storm Behavior, *Weather and Forecasting*, **10**, Issue 2, 449–453.
- [28] Cao, C. and Titi, E. S. 2005 *Global well-posedness of the three-dimensional primitive equations of large scale ocean and atmosphere dynamics* arXiv: Math. AP/0503028
- [29] Cao, C. and Titi, E. S. 2007 Global well-posedness of the three-dimensional primitive equations of large scale ocean and atmosphere dynamics, *Ann. Math.* **166**, 245–267.
- [30] Kobelkov, G. 2006 Existence of a solution “in whole” for the large-scale ocean dynamics equations, *Comptes Rendus Acad. Sci. Paris I*, **343**, 283–286.
- [31] Kobelkov, G. 2007 Existence of a Solution “in the large” for Ocean Dynamics Equations, *J. Math. Fluid Mech.* **9**, no. 4, 588–610.
- [32] Kobelkov, G., 2008 Existence and uniqueness of a solution to primitive equations with stratification in the large, *Russian J. Numer. Anal. Math. Modelling*, **23**, 39–61.
- [33] Ju, N. 2007 The global attractor for the solutions of the 3D viscous Primitive Equations, *Disc. Cont. Dyn. Systems*, **17**, 159–179.
- [34] Raugel, G. and Sell, G. R. 1993 Navier-Stokes equations on thin 3D domains I; Global attractors and global regularity of solutions, *J. Amer. Math. Soc.*, **6**, 503–568.
- [35] Raugel, G. and Sell, G. R. 1994 Navier-Stokes equations on thin 3D domains II; Global regularity of spatially periodic solutions, *Nonlinear partial differential equations and their applications*, Collège de France Seminar Vol XI, pp 205–247, Harlow: Longman Sci. Tech.

- [36] Hu, C., Temam, R. and Ziane, M. 2003 The primitive equations on the large scale ocean under the small depth hypothesis, *Discrete Contin. Dynam. Systems*, **9**, 97–131.
- [37] Lions, J., Temam, R. and Wang, S. 1992 New formulations of the primitive equations of atmosphere and applications, *Nonlinearity*, **5**, 237–288.
- [38] Lions, J., Temam, R. and Wang, S. 1992 On the equations of the large scale Ocean *Nonlinearity*, **5**, 1007–1053.
- [39] Lions, J., Temam, R. and Wang, S. 1995 Mathematical theory for the coupled atmosphere-ocean models, *J. Math. Pures Appl.*, **74**, 105–163.
- [40] Lewandowski, R. 2007 Résultat d'existence d'une solution faible au système des equations primitives, *Analyse Mathématique et océanographie: Essai sur la modélisation et l'analyse Mathématique de quelques modèles de turbulence utilisés en océanographie*, chapter 2, June 15.
- [41] Gibbon, J. D. 2009 Estimating intermittency in three-dimensional Navier-Stokes turbulence, *J. Fluid Mech.* **625**, 125–133.
- [42] Hide, R. 1964 The viscous boundary layer at the free surface of a rotating baroclinic fluid, *Tellus*, **16**, 523–529.
- [43] Hide, R. 1965 The viscous boundary layer at the free surface of a rotating baroclinic fluid: effects due to the temperature dependence of surface tension, *Tellus* **17**, 440–442.
- [44] Hide, R. 1969 Some laboratory experiments on free thermal convection in a rotating fluid subject to a horizontal temperature gradient and their relation to the global atmospheric circulation, pp 196–221 in *The Global Circulation of the Atmosphere* (ed. Corby G A), London: Royal Meteorological Society.